PLOS ONE

RESEARCH ARTICLE

Candida albicans PPG1, a serine/threonine phosphatase, plays a vital role in central carbon metabolisms under filament-inducing conditions: A multi-omics approach

Mohammad Tahseen A. L. Bataineh[1,2,3,4]*, Nelson Cruz Soares[2,5], Mohammad Harb Semreen[2,5], Stefano Cacciatore[6,7], Nihar Ranjan Dash[1], Mohamad Hamad[2,8], Muath Khairi Mousa[5], Jasmin Shafarin Abdul Salam[5], Mutaz F. Al Gharaibeh[1], Luiz F. Zerbini[6], Mawieh Hamad[2,8]*

1 College of Medicine, University of Sharjah, Sharjah, UAE, **2** Research Institute for Medical & Health Sciences at University of Sharjah, Sharjah, UAE, **3** Center for Biotechnology, Khalifa University of Science and Technology, Abu Dhabi, UAE, **4** Department of Genetics and Molecular Biology, College Of Medicine And Health Sciences, Khalifa University of Science and Technology, Abu Dhabi, UAE, **5** Department of Medicinal Chemistry, College of Pharmacy, University of Sharjah, Sharjah, UAE, **6** Cancer Genomics Group, International Centre for Genetic Engineering and Biotechnology, Cape Town, South Africa, **7** Institute for Reproductive and Developmental Biology, Imperial College, London, United Kingdom, **8** Department of Medical Laboratory Sciences, College of Health Sciences, University of Sharjah, Sharjah, UAE

* mohammad.bataineh@ku.ac.ae (MTALB); mabdelhaq@sharjah.ac.ae (MH)

Citation: A. L. Bataineh MT, Soares NC, Semreen MH, Cacciatore S, Dash NR, Hamad M, et al. (2021) *Candida albicans PPG1*, a serine/threonine phosphatase, plays a vital role in central carbon metabolisms under filament-inducing conditions: A multi-omics approach. PLoS ONE 16(12): e0259588. https://doi.org/10.1371/journal.pone.0259588

Editor: Yong-Sun Bahn, Yonsei University, REPUBLIC OF KOREA

Received: July 5, 2021

Accepted: October 21, 2021

Published: December 7, 2021

Peer Review History: PLOS recognizes the benefits of transparency in the peer review process; therefore, we enable the publication of all of the content of peer review and author responses alongside final, published articles. The editorial history of this article is available here: https://doi.org/10.1371/journal.pone.0259588

Abstract

Candida albicans is the leading cause of life-threatening bloodstream candidiasis, especially among immunocompromised patients. The reversible morphological transition from yeast to hyphal filaments in response to host environmental cues facilitates *C. albicans* tissue invasion, immune evasion, and dissemination. Hence, it is widely considered that filamentation represents one of the major virulence properties in *C. albicans*. We have previously characterized Ppg1, a PP2A-type protein phosphatase that controls filament extension and virulence in *C. albicans*. This study conducted RNA sequencing analysis of samples obtained from *C. albicans* wild type and *ppg1*Δ/Δ strains grown under filament-inducing conditions. Overall, *ppg1*Δ/Δ strain showed 1448 upregulated and 710 downregulated genes, representing approximately one-third of the entire annotated *C. albicans* genome. Transcriptomic analysis identified significant downregulation of well-characterized genes linked to filamentation and virulence, such as *ALS3*, *HWP1*, *ECE1*, *and RBT1*. *Expression analysis showed that essential* genes involved in *C. albicans* central carbon metabolisms, including *GDH3*, *GPD1*, *GPD2*, *RHR2*, *INO1*, *AAH1*, and *MET14* were among the top upregulated genes. Subsequent metabolomics analysis of *C. albicans ppg1*Δ/Δ strain revealed a negative enrichment of metabolites with carboxylic acid substituents and a positive enrichment of metabolites with pyranose substituents. Altogether, Ppg1 *in vitro* analysis revealed a link between metabolites substituents and filament formation controlled by a phosphatase to regulate morphogenesis and virulence.

Data Availability Statement: All relevant data are within the manuscript and its Supporting Information files.

Funding: MTA/1701090226-P, MH/1901050144, University of Sharjah, Sharjah, UAE. the Research Institute for Medical and Health Sciences, University of Sharjah UAE. This work was supported by research grants. The funders had no role in study design, data collection and analysis, decision to publish, or preparation of the manuscript.

Competing interests: The authors have declared that no competing interests exist.

Abbreviations: DEG, Differentially Expressed Genes; G.O., Gene Ontology; FDR, False Discovery Rate; PCA, Principal Component Analysis; W.T., Wild-Type; G.C.–M.S., Gas chromatography-mass spectrometric.

Introduction

Candida albicans is the most common opportunistic fungal pathogen in humans. It causes mucosal and systemic infections and is of medical significance due to its ability to cause hospital-acquired bloodstream infections with high mortality [1,2]. *C. albicans* is part of the normal flora of the oral cavity and the gastrointestinal and genitourinary tracts in healthy individuals. Immunocompromised hosts, including cancer patients on chemotherapy, organ transplant recipients, and patients with indwelling catheters, often develop disseminated candidiasis, a systemic form of the disease with close to 40% mortality [3–5]. Antifungal therapies available to treat systemic candidiasis are limited, and current therapies have adverse side effects [6,7].

C. albicans is a successful commensal with no known reservoirs outside the mammalian host and possesses multiple virulence properties that cause disease. A significant virulence property is the ability to undergo a dimorphic shift from single oval-shaped cells (yeast) into elongated cells attached end-to-end (pseudohyphal and hyphal filaments) in response to host environmental conditions [8–10]. Hyphal filaments are associated with virulence and virulence-related properties, including tissue invasion, lysis of macrophages and neutrophils, and breaching of endothelial cells [11–13]. Numerous genes expressed during the reversible morphogenic switch encode proteins that play crucial roles in virulence, such as secreted aspartic proteases (SAPs), which facilitate tissue damage, and adhesins, important for attachment of *C. albicans* to host surfaces [14,15]. Furthermore, transition to the hyphal form endows *C. albicans* with the ability to evade innate immunity [16]. Various host environmental stimuli induce *C. albicans* yeast-hyphal transition through a coordinated expression of transcriptional regulators influencing multiple signal transduction pathways, including the MAP kinase pathway and the Ras-cAMP-Protein Kinase A (PKA) pathway, among others [17]. During morphological switching, the activity of signaling pathway components is controlled by kinases and fine-tuned by phosphatases [18]. For example, *C. albicans* can survive harsh environmental conditions within the host owing to their ability to produce rapid and robust stress responses. Stress-activated protein kinase (SAPK) pathways tightly regulate these stress responses [19]. However, the contribution of phosphatases in fungal stress responses remains ambiguous.

Metabolic adaptation is vital for dimorphic switching in pathogenic yeast. During yeast to hyphal morphologic transition, *C. albicans* cells grown under hyphae-inducing conditions showed an overall downregulation of cellular metabolism and significant downregulation of carbon metabolism metabolic pathways [20]. Similarly, another metabolomic study performed with azole sensitive and resistant *C. albicans* strains identified a significant change in metabolic processes such as amino acid metabolism, tricarboxylic acid cycle, and phospholipid metabolism during the development of resistance to azole drugs [21]. Previous studies have shown that *Candida* strains deficient for *PPG1*, which encodes a putative serine/threonine PP2A phosphatase, remain locked in yeast or short germ tube forms and show reduced virulence mouse model of systemic candidiasis [22]. PP2A phosphatases help maintain cell wall integrity, actin cytoskeleton organization, auxin signaling in plant cells, polar movement, and mitophagy [23–26]. Although *PPG1* was previously reported to plays a vital role in *C. albicans* filament extension and virulence, its exact role in the multitude of transcriptional networks and signaling pathways that regulate fungal morphogenesis remains unclear. To gain more insight into the poorly understood role of phosphatases in controlling *C. albicans* filamentation and virulence, we performed a sequence-based analysis of RNA samples obtained from wild-type and *ppg1*Δ/Δ *C. albicans* cells grown under filament-inducing conditions as means of defining *PPG1*-related transcriptomic signatures. To complement our transcriptomics findings, we performed a detailed analysis of the metabolomic profiles of wild-type and *ppg1*Δ/Δ *C.*

albicans to understand further the bearing of *PPG1* on crucial metabolic pathways under different growth conditions.

Materials and methods

Strains, media, and culture conditions

Wild-type *C. albicans* (DK318) and *ppg1*Δ/Δ (MAY34) strains were used throughout this study as described previously [27]. Yeast extract-peptone-dextrose (YEPD) medium at 30˚C was used as the standard non-filament-inducing growth condition for all strains. Liquid serum and temperature induction experiments were performed by growing strains overnight in YEPD medium at 30˚C to an optical density at 600 nm (OD_{600}) of ∼4.0 and diluting 1:10 into 50 ml of prewarmed YEPD medium plus 10% serum at 37˚C as described previously [27]. Aliquots of cells harvested at specific post-induction time points 3 and 5 hours for RNA isolation. We selected 3 and 5 hours-time points as these times points show the most prominent phenotypic (filamentation) difference between *C. albicans* wild-type and *ppg1*Δ/Δ strains as shown before [28].

RNA isolation, purification, and sequencing

RNA extraction was performed using RNeasy Micro Kit (Qiagen GmbH, Germany), following the manufacturer's instructions. Three biological replicates were obtained for each condition (W.T. and mutant). RNA sequencing was performed at BGI Group, Shenzhen, China. RNA was extracted from 8 samples belonging to two different strains, DK318 and MAY34 are described in Table 1.

RNA sequencing and filtering

RNA obtained from 8 samples (Table 1) was sequenced using the BGISEQ-500 platform (Shenzhen, China), generating on average about 23.93 million reads per sample. The average mapping ratio with reference genomes was 96.92%, and the average gene mapping ratio was 82.77%; a total of 6,113 genes were detected. Sequence reads containing low-quality, adaptor-polluted and/or unknown high base (N) content were excluded from any further analysis. Retained sequence reads were further filtered using internal software SOAPnuke to produce a set of "clean reads" that was stored in FASTQ format as per each sample. Composition filtering statistics of raw data and quality metrics of clean reads are shown in S1 Table in S1 File.

Gene mapping analysis

Clean filtered sequence reads were mapped to the reference genome using HISAT (hierarchical indexing for spliced alignment of transcripts) to perform the genome mapping step. Reads

Table 1. Data description.

Sample ID	Description	Strain
PC3	*ppg1*Δ/Δ strain at 3 hrs. under 30˚C control	MAY34
PC5	*ppg1*Δ/Δ strain at 5 hrs. under 30˚C control	MAY34
PS3	*ppg1*Δ/Δ strain at 3 hrs. under 37˚C + serum	MAY34
PS5	*ppg1*Δ/Δ strain at 5 hrs. under 37˚C + serum	MAY34
WC3	Wild-type strain at 3 hrs. under 30˚C control	DK318
WC5	Wild-type strain at 5 hrs. under 30˚C control	DK318
WS3	Wild-type strain at 3 hrs. under 37˚C +serum	DK318
WS5	Wild-type strain at 5 hrs. under 37˚C +serum	DK318

https://doi.org/10.1371/journal.pone.0259588.t001

were mapped to the *C. albicans* strain SC5314 reference genome (assembly 21) (http://www.candidagenome.org). On average, 96.92% reads were mapped, and the uniformity of the mapping result for each sample suggested that the samples were comparable.

Gene expression analysis

Clean reads were mapped to reference transcripts using Bowtie2 [29] v2.2.5, and gene expression levels in each sample were calculated using RSEM [30] v1.2.12; mapping details are shown in S2 Table in S1 File.

Metabolite extraction and derivatization

The exact number of cells was used for each sample to avoid the effect of variable cell numbers. A volume of 300μL of the extraction solvent (acetonitrile: water, 1:1 v/v) was added to the cell pellets (2 million cells per pellet). The cells were then vortexed for 2 min to ensure the quantitative extraction of the metabolites and then stored in ice for one h, during which the samples were vortexed every 15 min. The insoluble cell matrices were then centrifuged (13,000 rpm, 10 min, −4˚C).

The supernatants were collected and transferred to G.C. vials for drying using EZ-2 Plus (GeneVac-Ipswich, UK) at 37 ± 1˚C. Polar metabolites such as amino acids and saccharides cannot be analyzed directly by G.C. due to their low volatility. Hence, it was necessary to derivatize them before the G.C.–M.S. analysis. The dry samples were dissolved in 25μL of 20 mg/mL methoxyamine hydrochloride in pyridine, followed by vortexing for 2 min, and stored for at least six h at 25˚C before the silylation step. Next, 25 μL of N-Methyl-N-(trimethylsilyl) trifluoroacetamide (MSTFA) + 1% Trimethylchlorosilane (TMCS) were added, which were then dissolved in 100 μL of pyridine and vortexed for 2 min. For complete derivatization, the samples were incubated at 50˚C for 30 min and then transferred to 200μL micro-inserts and analyzed by G.C.–M.S.

Gas chromatography-mass spectrometric analysis of the samples

G.C.–M.S. analysis was performed using a QP2010 gas chromatography-mass spectrometer (GC-2010 coupled with a G.C.–MS QP-2010 Ultra) equipped with an auto-sampler (AOC-20i +s) from Shimadzu (Tokyo, Japan), using Rtx-5ms column (30 m length × 0.25 mm inner diameter × 0.25 μm film thickness; Restek, Bellefonte, PA, USA). Helium (99.9% purity) was used as the carrier gas with a 1 mL/min column flow rate. The column temperature regime was initially adjusted at 35˚C for 2 min, followed by an increase in a rate of 10˚C/min to reach 250˚C. The temperature was then increased by 20˚C/min until reaching 320˚C and kept for 23 min. The injection volume and injection temperatures were 1 μL and 250˚C using splitless injection mode, respectively. The mass spectrometer operated in electron impact mode with electron energy of 70 eV. The ion source temperature and the interface temperature were set at 240˚C and 250˚C, respectively. The MS mode was set on scan mode starting from 50–650 m/z with a scan speed of 1428. Data collection and analysis were performed using MSD Enhanced Chemstation software (Shimadzu). G.C. total ion chromatograms (TIC) and fragmentation patterns of the compound were identified using the NIST/EPA/NIH Mass Spectral Library (NIST 14) (S1 File). The run time for each sample was 43.67 min [31].

Preprocessing gas chromatography-mass spectrometry (GC-MS) data

Preprocessing of metabolomics data was performed using an in-house R script. Probabilistic Quotient Normalization [32] normalizes data due to dilution effects in the extraction

procedure using the function normalization in the R package KODAMA [33]. The number of missing metabolites in the three replicates of each condition (i.e., drug and cell line) was counted. When the number was equal to 3, missing values were imputed with zero; otherwise, missing values were imputed using the k-nearest neighbor (kNN) algorithm [34], with k = 2. By limiting the kNN imputation to the metabolites with at least two values out of 3/condition, imputation using the information from different conditions (e.g., treated and non-treated) was avoided.

Data analysis and statistical approach

DEGseq [35] and PossionDis [36] algorithms were used to detect the differentially expressed genes (DEG) between samples and groups. Hierarchical clustering for DEGs was performed using the R function heatmap. Mfuzz [37] v2.34.0 was used to cluster gene expression data for time series. Overrepresentation analysis (ORA) was used to determine the gene ontology (G. O.) functional enrichment of DEGs using the hypergeometric test using the R function phyper. Then we calculate the false discovery rate (FDR) for each p-value. In general, it was defined as significantly enriched in terms where FDR was not larger than 0.01. Principal component analysis (PCA) was used to visualize the metabolomic data. Data were mean-centered and scaled to unit variance before PCA. Metabolite set enrichment analysis (MSEA) was carried out using the Gene Set Enrichment Analysis (GSEA) algorithm [38]. The metabolite sets were built using the substituents characterization provided by the Human Metabolome Database [39]. The ranking in the MSEA was performed by using the coefficient of the first principal component of PCA. Two-way ANOVA was used to compare the strains, treatment and to investigate their interaction. The threshold for significance was $p < 0.05$ to account for multiple testing, a false discovery rate (FDR) was calculated using the q conversion algorithm in multiple comparisons. For metabolomics analysis, an FDR of <5% was chosen to reduce the identification of false positives. All data, including the raw QGD files, has been deposited to Metabolomics Workbench (https://www.metabolomicsworkbench.org). The data track ID is 2026.

Results

Transcriptomic changes in the C. albicans ppg1Δ/Δ strain growing under strong filament-inducing conditions

The pattern of gene expression in wild-type (DK318) and *ppg1*Δ/Δ (MAY34) strains of *C. albicans* growing under filament-inducing (10% fetal bovine serum at 37˚C) at different time points post culture (3 and 5 hours) was investigated as means of tracking any transcriptional changes that occur during the morphological transition from yeast to hyphae. The filamentation phenotype of both wild-type (W.T.) and *ppg1*Δ/Δ *C. albicans* strains under filamentation induction conditions was confirmed microscopically and was consistent with previously published observations [28]. As expected, all cells grew as yeast at the 37˚C non-inducing control condition, just before induction and their gene expression profile shows comparable results between *ppg1*Δ/Δ and W.T. strains. A Scatter plot of DEGs analyses of the RNA sequencing data was used to visualize the transcriptomic changes. The *ppg1*Δ/Δ strain relative to W.T. (W. S. *vs*. P.S.) at 5 hours post-induction with serum at 37˚C and showed a significant effect for *ppg1*Δ/Δ mutation on *C. albicans* gene expression at the 5-hour time point, genes that showed >2-fold change in expression levels were considered as differentially expressed. A total of 2,158 genes showed a significant difference in expression between WS5 and PS5 (Fig 1A), more detalied information can be found at the S1 File. Based on these parameters, 1448 DEGs were upregulated, and 710 were downregulated in the *ppg1*Δ/Δ samples relative to W.T.

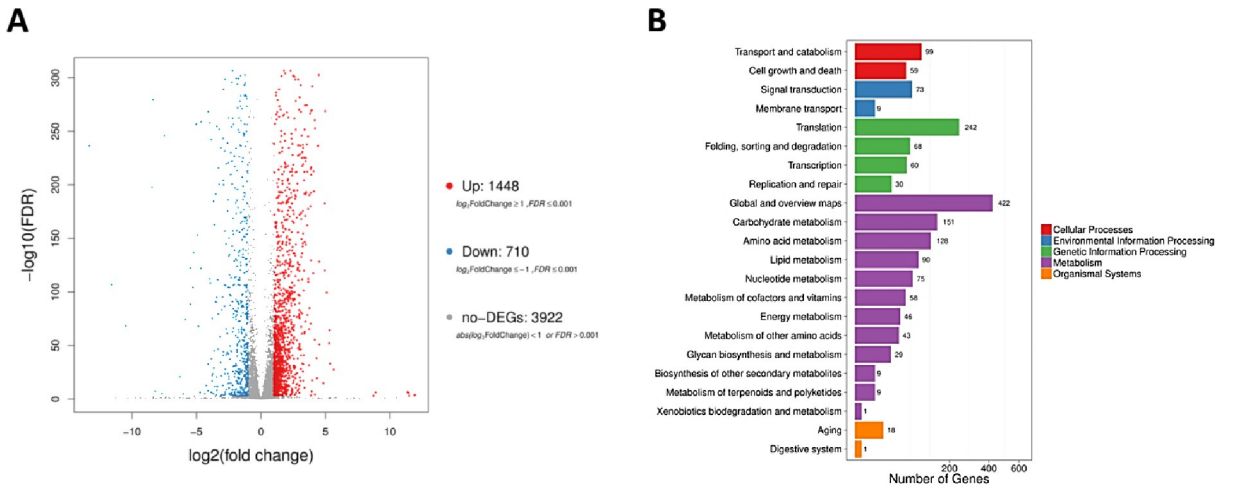

Fig 1. Transcriptomic changes of *C. albicans ppg1*Δ/Δ strain growing under strong filament-inducing condition, 10% serum at 37˚C. (A) Scatter plots of DEGs, X and Y axes represent $\log_{10}$ transformed gene expression level, red color represents significantly upregulated genes, and blue color represents significantly down-regulated genes in W.S. and P.S. at the 5 hr. time point. (B) Pathway classification of DEGs. The X-axis represents the number of DEG. Y-axis represents the functional classification of KEGG. There are seven KEGG pathways: Cellular Processes, Environmental Information Processing, Genetic Information Processing, Metabolism, Organismal Systems.

https://doi.org/10.1371/journal.pone.0259588.g001

control at the 5 hr. time point. We further classified the identified DEGs according to the proposed functional pathway, 1061 DEGs identified under metabolism KEGG pathways (Fig 1B).

PPG1 modulates the expression of multiple filament-specific and central carbon metabolisms genes in response to serum at 37˚C: To identify essential gene targets affected by *PPG1*, we examined genes with a four-fold or more change expression between W.S. and P.S. (Table 2).

This list of genes included filament-specific genes such as *ALS3*, *HWP1*, *ECE1*, *RBT1*, and genes involved in *C. albicans* central carbon metabolisms such as *GDH3*, *GPD1*, *GPD2*, *RHR2*, *INO1*, *AAH1*, and *MET14*.

We further explored top enriched G.O. terms from DEGs based on various metabolic processes and signaling pathways. To further explore the effect of *PPG1* on various biological

Table 2. List of selected gene targets with a four-fold or more change in expression in *ppg1* Δ/Δ strain.

Gene Symbol	log2 Fold Change	P-Value	FDR	Gene Function
GDH3	7.77957	0.000	0.000	oxidoreductase activity, acting on the CH-NH2 group of donors, NAD or NADP as acceptor glutamate dehydrogenase (NADP+) activity
INO1	7.202084	0.000	0.000	inositol-3-phosphate synthase activity phospholipid biosynthetic process
AAH1	5.312624	1.14E-65	5.10E-65	metal ion binding adenine deaminase activity
GPD2	4.991099	0.000	0.000	NAD binding protein homodimerization activity
MET14	4.75566	0.000	0.000	ATP binding adenylylsulfate kinase activity
GPD1	4.688903	0.000	0.000	NAD binding protein homodimerization activity
RHR2	4.653127	0.000	0.000	hydrolase activity glycerol-3-phosphatase activity
JEN2	-13.4639	0.000	0.000	dicarboxylic acid transmembrane transporter activity transmembrane transporter activity
HWP1	-5.2734	1.03E-105	6.22E-105	hyphal cell wall adhesion molecule binding
ECE1	-4.84915	3.54E-69	1.66E-69	hypha-specific protein with toxin activity
ALS3	-4.80271	1.16E-19	2.81E-19	agglutinin-like sequence adhesins
RBT1	-4.452919	1.49E-19	1.97E-06	cell wall protein

https://doi.org/10.1371/journal.pone.0259588.t002

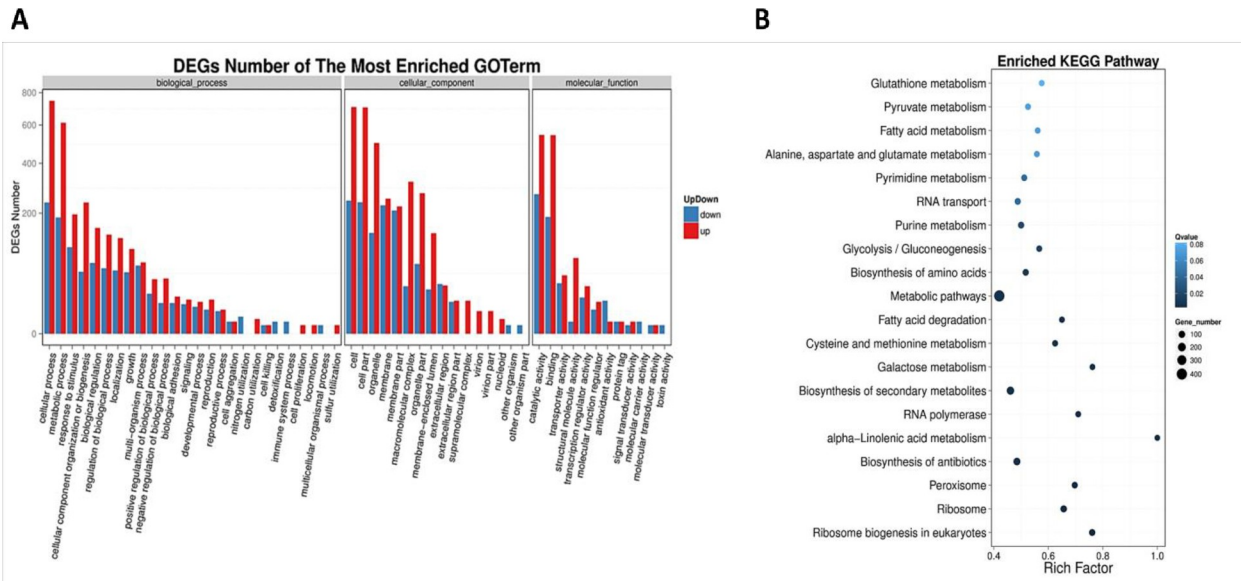

Fig 2. Global transcriptomic analysis and pathway functional enrichment of DEGs in *C. albicans ppg1* Δ/Δ strain growing under strong filament-inducing condition. (A) Bar graph representation of significantly up/down-regulated genes, X-axis, represents G.O. term. Y-axis represents the amount of retained G.O. terms for biological processes in RNA sequencing analysis in response to filament-induction. (B) The X-axis represents the enrichment factor. Y-axis represents the pathway name. Rich Factor refers to the value of enrichment factor, the quotient of foreground value (the number of DEGs), and background value (total gene amount). The larger the value, the more significant enrichment.

https://doi.org/10.1371/journal.pone.0259588.g002

functions, we determined the functional pathway enrichment of DEGs (Fig 2A). In order to detect which metabolic pathways were affected by *PPG1*, we conducted a Kyoto Encyclopedia of Genes and Genomes (KEGG) analysis. This analysis detected a total of 20 enriched KEGG pathways that were significantly downregulated in *C. albicans ppg1*Δ/Δ strain growing under filament-inducing conditions (Fig 2B). The data showed significant enrichment of multiple metabolic pathways, such as those involved in sugar (galactose) (P-value 0.0003, FDR 3.965E-03), amino acid (P-value 0.0009, FDR 8.7187E-03), nucleotide (purines) (P-value 0.0023, FDR 1.987E-02), and fatty acid (alpha-linolenic acid) metabolism (P-value 9.357E-05, FDR 2.795E-03) among others (Fig 2B).

Metabolomics analysis of C. albicans ppg1Δ/Δ strain growing under strong filament-inducing. Using GC-MS, we profiled 35 metabolites (15 sugars and 20 amino acids). First, we examined the variance in the metabolic profiles among different samples using PCA (Fig 3A).

The first component (PC1) accounted for 34.5% of the total variance in the data set, with a further 22.2% explained by the second component (PC2). In the first component, we noted that the serum treatment had a considerable effect on the metabolic profile of the W.T. strains. However, this effect was not observable in the treatment of the *ppg1*Δ/Δ strain. Then, we performed enrichment analysis on the metabolites that contributed to determining the first principal component scores using their substituent characterization. According to the pre-ranked MSEA based on the first principal component's coefficient, we observed a negative enrichment of metabolites with carboxylic acid substituents (p-value = $5.75x10^{-3}$; FDR = $1.32x10^{-2}$) and a positive enrichment of metabolites with pyranose substituents (p-value = $5.60x10^{-2}$; FDR = $4.47x10^{-1}$). More detailed results of the 26 substituents metabolite sets are provided in Table 3. Further, we did not detect a significant difference between both strains at non-inducing control conditions.

Among the metabolites included in the carboxylic acid substituent group, we observed a statistically significant interaction between genotype (*ppg1*Δ/Δ, W.T. strains) and treatment

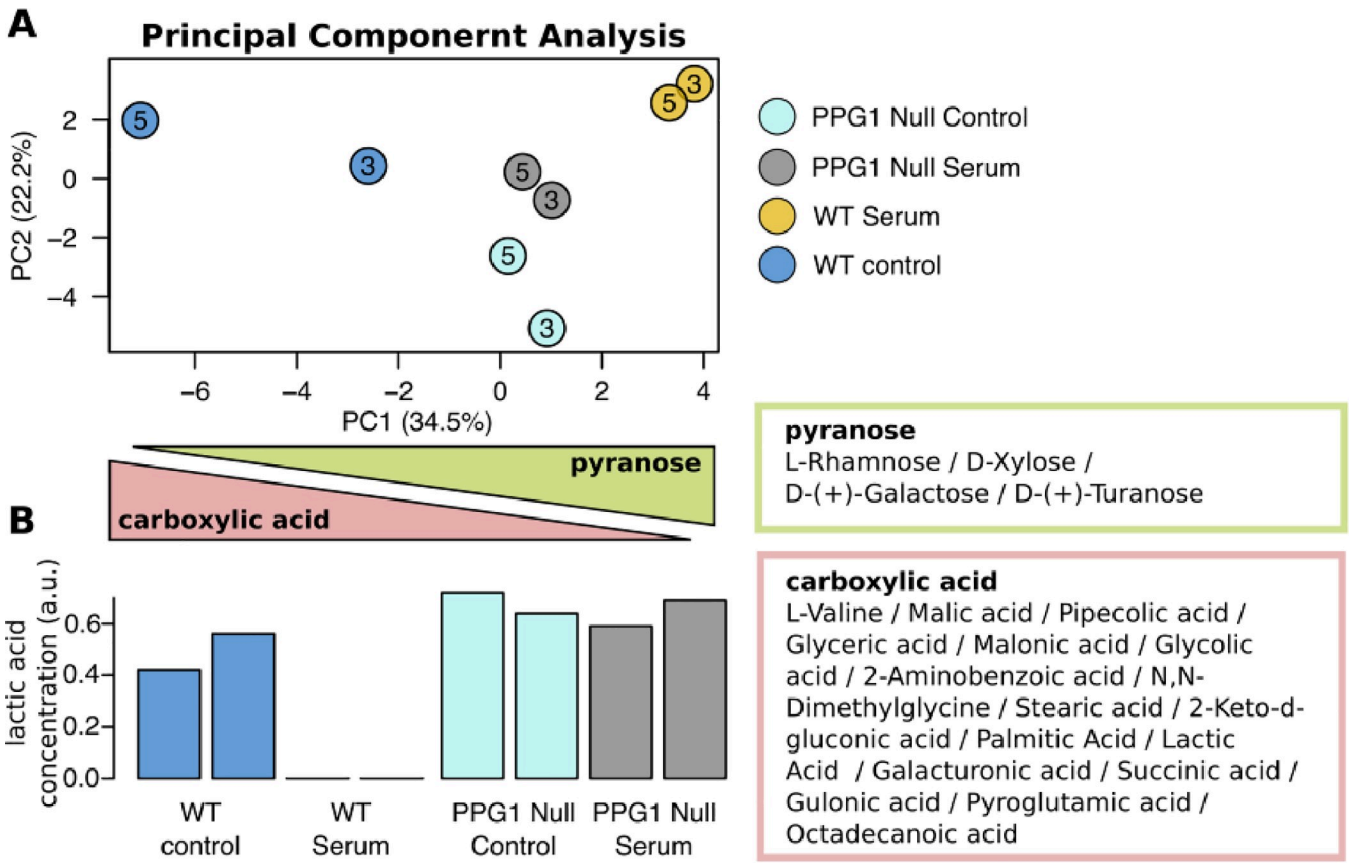

Fig 3. (A) PCA of the metabolomics profile in *C. albicans* under filament-inducing (10% fetal bovine serum at 37˚C) and control for wild-type *C. albicans* (DK318) and *ppg1*Δ/Δ (MAY 34) strains. Cells were harvested at three and five hours. (B) The relative concentration of lactic acid. PC1 = first principal component; PC2 = second principal component.

https://doi.org/10.1371/journal.pone.0259588.g003

with (serum at 37˚C) on the lactic acid levels (p-value = $1.77x10^{-2}$; FDR = $1.27x10^{-1}$) using ANOVA. Indeed, we observed a complete depletion of lactic acid only in the W.T. strain when treated with serum (Fig 3B). ANOVA analysis on all metabolites is reported in S3 Table in S1 File.

Discussion

Phosphorylation is an essential post-translational modification step that is highly conserved across all eukaryotes' signaling events. In *Candida*, kinases drive most cellular biologic functions, including metabolism, filamentation, and virulence [40]. Phosphatase (dephosphorylation) counters incessant kinase activity and maintains cellular homeostasis in response to different environmental stimuli [41]. This study provides new insight into the contribution of phosphatases in *C. albicans* morphogenesis utilizing transcriptomic and metabolomics approaches. Ppg1, a serine/threonine protein phosphatase, plays a vital role in controlling *C. albicans* morphology and virulence [28]. To further explore the poorly understood role of phosphateses in *C albicans* morphology and virulence, we carried out detailed transcriptomic and metabolomics profiling of wild-type and ppg1 mutants strains of the pathogen. The data showed that *C. albicans ppg1* Δ/Δ strain growing under strong filament-inducing conditions undergo significant transcriptomic changes. The hierarchical clustering and scatter plot of DEGs showed changes in >35% of the entire *Candida* genome, 1448 upregulated genes, and

Table 3. List of metabolites associated with Ppg1.

pathway	p-value	FDR	ES	NES	size	metabolites
Carboxylic acid	5.75E-03	1.32E-01	-0.75	-1.77	17	L-Valine/Malic acid/Pipecolic acid/Glyceric acid/Malonic acid/Glycolic acid/ 2-Aminobenzoic acid/N,N-Dimethylglycine/Stearic acid/2-Keto-d-gluconic acid/Palmitic Acid/Lactic Acid/Galacturonic acid/Succinic acid/Gulonic acid/Pyroglutamic acid/ Octadecanoic acid
Pyranose	5.60E-02	4.47E-01	0.85	1.74	4	L-Rhamnose/D-Xylose/D-(+)-Galactose/D-(+)-Turanose
Beta-hydroxy acid	6.61E-02	4.47E-01	-0.80	-1.41	4	Malic acid/Glyceric acid/Galacturonic acid/Gulonic acid
Polyol	8.16E-02	4.47E-01	0.45	1.39	12	Pentitol/Glycerol/2-Keto-d-gluconic acid/L-Rhamnose/Galacturonic acid/D-Xylose/D-(+)-Galactose/Gulonic acid/Scyllo-Inositol/D-(+)-Turanose/Xylitol/Myo-Inositol
Oxacycle	1.17E-01	4.47E-01	0.60	1.38	5	Uridine/L-Rhamnose/D-Xylose/D-(+)-Galactose/D-(+)-Turanose
Amino acid	1.18E-01	4.47E-01	-0.74	-1.31	4	L-Valine/Pipecolic acid/2-Aminobenzoic acid/N,N-Dimethylglycine
Dicarboxylic acid or derivatives	1.36E-01	4.47E-01	-0.80	-1.29	3	Malic acid/Malonic acid/Succinic acid
Fatty acid	1.81E-01	5.20E-01	-0.61	-1.25	7	L-Valine/Malic acid/Galacturonic acid/Succinic acid/Gulonic acid/Palmitic Acid/ Octadecanoic acid
Carbonyl group	2.34E-01	5.40E-01	-0.51	-1.21	19	L-Valine/Malic acid/Pipecolic acid/Glyceric acid/Malonic acid/Glycolic acid/N, N-Dimethylglycine/Stearic acid/2-Keto-d-gluconic acid/Palmitic Acid/Lactic Acid/Glycerol monostearate/Galacturonic acid/Succinic acid/Gulonic acid/Pyroglutamic acid/Oleic acid amide/D-(+)-Turanose/Octadecanoic acid
Alpha-hydroxy acid	2.35E-01	5.40E-01	-0.61	-1.20	6	Malic acid/Glyceric acid/Glycolic acid/Lactic Acid/Galacturonic acid/Gulonic acid
Carboxylic acid derivative	3.12E-01	6.27E-01	-0.49	-1.13	13	Malic acid/Glyceric acid/Glycolic acid/2-Aminobenzoic acid/Stearic acid/2-Keto-d-gluconic acid/Palmitic Acid/Lactic Acid/Glycerol monostearate/Galacturonic acid/Gulonic acid/Oleic acid amide/Octadecanoic acid
Fatty acyl	3.48E-01	6.27E-01	-0.62	-1.09	4	L-Valine/Glycerol monostearate/Galacturonic acid/Gulonic acid
Sugar alcohol	3.54E-01	6.27E-01	0.45	1.03	5	Pentitol/Glycerol/Scyllo-Inositol/Xylitol/Myo-Inositol
Alcohol	4.41E-01	7.25E-01	-0.43	-1.03	20	Ergosterol/Octadecanol/Pentitol/Malic acid/Glyceric acid/Glycolic acid/Glycerol/2-Keto-d-gluconic acid/Lactic Acid/Glycerol monostearate/Uridine/Acetoin/Tryptophol/L-Rhamnose/ Galacturonic acid/D-Xylose/D-(+)-Galactose/Gulonic acid/D-(+)-Turanose/Xylitol
Organonitrogen compound	5.52E-01	8.47E-01	-0.46	-0.96	8	L-Valine/Pipecolic acid/2-Aminobenzoic acid/N,N-Dimethylglycine/Uridine/Tryptophol/ Pyroglutamic acid/Oleic acid amide
Primary alcohol	6.69E-01	8.98E-01	-0.37	-0.86	13	Octadecanol/Pentitol/Glyceric acid/Glycolic acid/Glycerol/2-Keto-d-gluconic acid/Glycerol monostearate/Uridine/Tryptophol/D-(+)-Galactose/Gulonic acid/D-(+)-Turanose/Xylitol
Monosaccharide	6.87E-01	8.98E-01	-0.44	-0.86	6	Pentitol/Glyceric acid/Uridine/Galacturonic acid/Gulonic acid/Xylitol
Cyclic alcohol	7.14E-01	8.98E-01	-0.53	-0.85	3	Ergosterol/Scyllo-Inositol/Myo-Inositol
Azacycle	7.55E-01	8.98E-01	-0.47	-0.83	4	Pipecolic acid/Uridine/Tryptophol/Pyroglutamic acid
Ketone	8.13E-01	8.98E-01	0.41	0.74	3	2-Keto-d-gluconic acid/Acetoin/D-(+)-Turanose
Secondary alcohol	8.20E-01	8.98E-01	-0.30	-0.72	17	Ergosterol/Pentitol/Malic acid/Glyceric acid/Glycerol/2-Keto-d-gluconic acid/Lactic Acid/ Uridine/2,3-Butanediol/Acetoin/L-Rhamnose/Galacturonic acid/D-Xylose/D-(+)-Galactose/ Gulonic acid/D-(+)-Turanose/Xylitol
Aliphatic heteromonocyclic compound	8.79E-01	9.19E-01	-0.34	-0.67	6	Pipecolic acid/L-Rhamnose/D-Xylose/D-(+)-Galactose/Pyroglutamic acid/D-(+)-Turanose
Organoheterocyclic compound	9.82E-01	9.82E-01	-0.26	-0.53	7	Pipecolic acid/Uridine/L-Rhamnose/D-Xylose/D-(+)-Galactose/Pyroglutamic acid/D-(+)-Turanose

Abbreviations: ES = enrichment score; NES = normalized enrichment score; FDR = false discovery rate.

https://doi.org/10.1371/journal.pone.0259588.t003

710 downregulated genes compared to the W.T. control. Consistent with previous findings, this significant transcriptional change suggests an important, and possibly a master regulator, the role of *PPG1* in filament extension, among other potential roles [28,41,42]. *PPG1* role is not surprising given that ser/thr phosphatases consist of multiprotein complexes with significant structural diversity that provides for an expansive array of regulatory roles in multiple signaling events.

Among the critical targets for the Ppp1 regulatory effect were filament-specific and central carbon metabolism pathways. Consistent with the previous analysis, the most downregulated genes in *ppg1* Δ/Δ *C. albicans* grown at 37˚C were genes involved in filamentation and virulence, such as *ALS3*, *HWP1*, *ECE1*, and *RBT1* [43]. It is well accepted that *C. albicans* cells utilize Als3 (a member of the agglutinin-like sequence adhesins) during filamentation for epithelial adhesion [44]. Moreover, Als3 plays a significant role in iron acquisition, which is critical for fungal pathogenesis [45]. Interestingly, we noticed an upregulation in the expression of the iron transport gene *FET31* in *C. albicans ppg1*Δ/Δ strain. *FET31* upregulation could reflect increased metabolism [46] in the *ppg1*Δ/Δ strain as suggested by the transcriptomic profile shown in Figs 1 and 2. Furthermore, our data suggest that *PPG1* could function as a significant regulator given that it increased the expression of multiple carbon metabolism genes, including *GDH3*, *GPD1*, *GPD2*, *RHR2*, *INO1*, *AAH1*, and *MET14*. *GDH3* (NADPH-dependent glutamate dehydrogenase). This group of genes is collectively essential for nitrogen metabolism, the maintenance of the redox balance, and *C. albicans* filament formation [47,48]. For example, *GPD1* and *GPD2* (two isoforms of glycerol 3-phosphate dehydrogenase) are rate-controlling enzymes in essential glycerol formation reactions in *Saccharomyces cerevisiae* [49]. They also play a crucial role in osmoregulation, carbohydrate metabolism, and redox balancing [47,50]. It is worth noting that both Gpd1 and Gpd2 are negatively regulated by the phosphorylation activity of the AMP-activated protein kinase Snf1, the TORC2-dependent kinases Ypk1 and Ypk2 possibly in a Ppg1-dependant manner [51]. Additionally, Candida glycerol 3-phosphate dehydrogenases help the pathogen evade the immune response through their ability to interact with the vital complement regulators, including H and H–like factors [52]. *RHR2* (glycerol 3-phosphatase) is also essential for osmotic stress, glycerol accumulation, biofilm formation, and yeast-hyphal switch [53,54]. *INO1* (Inositol-1-phosphate synthase), which is vital for inositol synthesis, is considered as a growth factor that supports the formation of glycophosphatidylinositol (GPI)-anchored glycolipids on *Candida* cell surface and hence the promotion of pathogenesis [55,56]. *AAH1* (an Adenine deaminase) is similar to serine/threonine dehydratases essential for purine salvage and nitrogen catabolism [47]. *MET14* (an adenylylsulfate kinase) is essential for assimilating sulfate to sulfide, which strongly depends on yeast growth conditions such as glucose [57].

Our data showed that a total of 20 enriched KEGG pathways were significantly downregulated in *C. albicans ppg1*Δ/Δ strain growing under filament-inducing conditions (Fig 2B). These mainly included pathways involved in sugars (galactose) and amino acid biosynthesis and purine metabolism, all of which are essential for filament extension and virulence [58,59]. Interestingly, the highest pathway enrichment in *C. albicans ppg1*Δ/Δ strain grown under filament growth conditions concerns the metabolism of alpha-Linolenic acid (ALA), a known inhibitor of hyphal growth *C. albicans*. Previous transcriptional profiling revealed that ALA downregulates hypha-specific genes in a *UME6* and *RFG1* (hyphal transcriptional regulators) independent manner. Perhaps ALA functions through a Ppg1- dependent mechanism [60].

Based on the above-noted discussion, we sought to explore further the effect of *PPG1* on *C. albicans* metabolic functions using GC-MS metabolomics analysis. We profiled 35 metabolites, including sugars and amino acids. Enrichment analysis showed an adverse enrichment profile of metabolites with carboxylic acid substituents in *C. albicans ppg1*Δ/Δ strain growing under strong filament-inducing conditions and consistent with the downregulation of Jen2 (a dicarboxylic acid transporter protein), which was previously shown to be regulated by glucose repression in *C. albicans* as shown in Table 1 [61]. *C. albicans* uses carboxylic acids substituents including acetate and lactate for survival and evasion of phagocytosis [62,63]. For example, macrophages-mediated phagocytosis during systemic candidiasis in mice was reported to induce lactate and acetate transporters [63]. Positive enrichment of metabolites with pyranose

substituents in *C. albicans ppg1*Δ/Δ strain growing under strong filament-inducing conditions consistent with the upregulation of genes involved in central carbon metabolism and hence fungal pathogenicity [47]. Glycans are critical for fungal pathogenesis owing to their well-established roles in cell adhesion, immune cell evasion, and inhibition of lymphoproliferation [64–66]. Mannans as a vital component of the fungal cell wall, are also of significance in fungal virulence; inactivation of genes involved in mannan biosynthesis was previously linked to decreased virulence of *C. albicans* [67]. Altogether, Ppg1 seems to exhibit a master regulator role that influences lactic acid and carboxylic acid utilization and the conversion of pyranose to sugars that could be utilized to synthesize filamentation-related cell wall polysaccharides.

In conclusion, the data presented here elaborated on the role of phosphatases such as *PPG1* in regulating the morphological transition of *C. albicans* at the transcriptional level. *PPG1* affected the expression of >35% of the *Candida* genus, especially those involved in or associated with *C. albicans* pathogenesis, filamentation, and metabolic activities. Shedding more light on the regulatory events that ensue during *C. albicans* filamentous growth and virulence may lead to novel antifungal therapeutic strategies. Further work is still needed to validate the findings presented by this study using *PPG1* mutant-induced animal models. Further analysis of the role of Ppg1 in protein glycosylation and other virulence-related events such as biofilm formation and immune evasion is also warranted.

Supporting information

S1 File. Supporting file contains all the supporting tables and figures, supplementary file.
S1 Fig. GC-MS total ion chromatograms (TIC) of metabolites extract from *Candida albicans*.
S1 Table. Clean reads quality metrics. S2 Table. Summary of Genome Mapping Ratio. S3 Table. Metabolites interplay between *ppg1*Δ/Δ and W.T. strains.
(XLSX)

Acknowledgments

We are grateful to David Kadosh (U.T. Health, San Antonio), USA, to provide *C. albicans* strains.

Author Contributions

Conceptualization: Mohammad Tahseen A. L. Bataineh, Nelson Cruz Soares, Mawieh Hamad.

Data curation: Mohammad Tahseen A. L. Bataineh, Mohammad Harb Semreen, Stefano Cacciatore, Muath Khairi Mousa, Jasmin Shafarin Abdul Salam.

Formal analysis: Mohammad Tahseen A. L. Bataineh, Nelson Cruz Soares, Mohammad Harb Semreen, Stefano Cacciatore, Nihar Ranjan Dash, Mohamad Hamad, Muath Khairi Mousa, Mawieh Hamad.

Funding acquisition: Mohammad Tahseen A. L. Bataineh, Mawieh Hamad.

Investigation: Mohammad Tahseen A. L. Bataineh, Nelson Cruz Soares, Nihar Ranjan Dash, Jasmin Shafarin Abdul Salam, Mawieh Hamad.

Methodology: Mohammad Tahseen A. L. Bataineh, Nelson Cruz Soares, Mohammad Harb Semreen, Nihar Ranjan Dash, Muath Khairi Mousa, Jasmin Shafarin Abdul Salam, Mawieh Hamad.

Resources: Mohammad Tahseen A. L. Bataineh, Nelson Cruz Soares, Mohammad Harb Semreen, Stefano Cacciatore, Muath Khairi Mousa, Luiz F. Zerbini, Mawieh Hamad.

Software: Nelson Cruz Soares, Mohammad Harb Semreen, Stefano Cacciatore, Mohamad Hamad, Muath Khairi Mousa, Jasmin Shafarin Abdul Salam, Mutaz F. Al Gharaibeh, Luiz F. Zerbini, Mawieh Hamad.

Supervision: Mohammad Tahseen A. L. Bataineh, Mohammad Harb Semreen, Nihar Ranjan Dash, Mohamad Hamad, Luiz F. Zerbini, Mawieh Hamad.

Validation: Mohammad Tahseen A. L. Bataineh, Nelson Cruz Soares.

Visualization: Stefano Cacciatore, Mutaz F. Al Gharaibeh.

Writing – original draft: Mohammad Tahseen A. L. Bataineh, Nelson Cruz Soares, Mohammad Harb Semreen, Stefano Cacciatore, Nihar Ranjan Dash, Mohamad Hamad, Muath Khairi Mousa, Jasmin Shafarin Abdul Salam, Mutaz F. Al Gharaibeh, Luiz F. Zerbini, Mawieh Hamad.

Writing – review & editing: Mohammad Tahseen A. L. Bataineh, Nelson Cruz Soares, Mohammad Harb Semreen, Stefano Cacciatore, Nihar Ranjan Dash, Mohamad Hamad, Muath Khairi Mousa, Jasmin Shafarin Abdul Salam, Mutaz F. Al Gharaibeh, Luiz F. Zerbini, Mawieh Hamad.

References

1. Edmond MB, Wallace SE, McClish DK, Pfaller MA, Jones RN, Wenzel RP. Nosocomial bloodstream infections in United States hospitals: a three-year analysis. Clinical infectious diseases: an official publication of the Infectious Diseases Society of America. 1999; 29(2):239–44. Epub 1999/09/07. https://doi.org/10.1086/520192 PMID: 10476719.
2. Wisplinghoff H, Bischoff T, Tallent SM, Seifert H, Wenzel RP, Edmond MB. Nosocomial bloodstream infections in U.S. hospitals: analysis of 24,179 cases from a prospective nationwide surveillance study. Clinical infectious diseases: an official publication of the Infectious Diseases Society of America. 2004; 39(3):309–17. Epub 2004/08/13. https://doi.org/10.1086/421946 PMID: 15306996.
3. Odds F.C. Pathogenesis of Candida infections. Journal of the American Academy of Dermatology. 1994; 31(3 Pt 2):S2–5. Epub 1994/09/01. https://doi.org/10.1016/s0190-9622(08)81257-1 PMID: 8077502.
4. Mayer FL, Wilson D, Hube B. Candida albicans pathogenicity mechanisms. Virulence. 2013; 4(2):119–28. Epub 2013/01/11. https://doi.org/10.4161/viru.22913 PMID: 23302789; PubMed Central PMCID: PMC3654610.
5. Hebecker B, Naglik JR, Hube B, Jacobsen ID. Pathogenicity mechanisms and host response during oral Candida albicans infections. Expert review of anti-infective therapy. 2014; 12(7):867–79. Epub 2014/05/08. https://doi.org/10.1586/14787210.2014.916210 PMID: 24803204.
6. Hartland CL, Youngsaye W, Morgan B, Ting A, Nag P, Buhrlage S, et al. Identification of small molecules that selectively inhibit fluconazole-resistant Candida albicans in the presence of fluconazole but not in its absence—Probe 2. Probe Reports from the NIH Molecular Libraries Program. Bethesda (MD) 2010.
7. Scorzoni L, de Paula ESAC, Marcos CM, Assato PA, de Melo WC, de Oliveira HC, et al. Antifungal Therapy: New Advances in the Understanding and Treatment of Mycosis. Frontiers in microbiology. 2017; 8:36. Epub 2017/02/09. https://doi.org/10.3389/fmicb.2017.00036 PMID: 28167935; PubMed Central PMCID: PMC5253656.
8. Biswas S, Van Dijck P, Datta A. Environmental sensing and signal transduction pathways regulating morphopathogenic determinants of Candida albicans. Microbiology and molecular biology reviews: MMBR. 2007; 71(2):348–76. Epub 2007/06/08. https://doi.org/10.1128/MMBR.00009-06 PMID: 17554048; PubMed Central PMCID: PMC1899878.
9. Mitchell AP. Dimorphism and virulence in Candida albicans. Current opinion in microbiology. 1998; 1 (6):687–92. Epub 1999/03/06. https://doi.org/10.1016/s1369-5274(98)80116-1 PMID: 10066539.
10. Grainha TRR, Jorge P, Perez-Perez M, Perez Rodriguez G, Pereira M, Lourenco AMG. Exploring anti-quorum sensing and anti-virulence based strategies to fight Candida albicans infections: an in silico

approach. FEMS yeast research. 2018;18(3). Epub 2018/03/09. https://doi.org/10.1093/femsyr/foy022 PMID: 29518242.

11. Sherwood J, Gow NA, Gooday GW, Gregory DW, Marshall D. Contact sensing in Candida albicans: a possible aid to epithelial penetration. Journal of medical and veterinary mycology: bi-monthly publication of the International Society for Human and Animal Mycology. 1992; 30(6):461–9. Epub 1992/01/01. https://doi.org/10.1080/02681219280000621 PMID: 1287165.

12. Mu C, Pan C, Han Q, Liu Q, Wang Y, Sang J. Phosphatidate phosphatase Pah1 has a role in the hyphal growth and virulence of Candida albicans. Fungal genetics and biology: FG & B. 2019; 124:47–58. Epub 2019/01/08. https://doi.org/10.1016/j.fgb.2018.12.010 PMID: 30615943.

13. Kumamoto CA, Vinces MD. Contributions of hyphae and hypha-co-regulated genes to Candida albicans virulence. Cellular microbiology. 2005; 7(11):1546–54. Epub 2005/10/07. https://doi.org/10.1111/j.1462-5822.2005.00616.x PMID: 16207242.

14. Aoki W, Kitahara N, Miura N, Morisaka H, Yamamoto Y, Kuroda K, et al. Comprehensive characterization of secreted aspartic proteases encoded by a virulence gene family in Candida albicans. Journal of biochemistry. 2011; 150(4):431–8. Epub 2011/06/08. https://doi.org/10.1093/jb/mvr073 PMID: 21646240.

15. Sturtevant J, Calderone R. Candida albicans adhesins: Biochemical aspects and virulence. Revista iberoamericana de micologia. 1997; 14(3):90–7. Epub 2007/07/28. PMID: 17655381.

16. Duhring S, Germerodt S, Skerka C, Zipfel PF, Dandekar T, Schuster S. Host-pathogen interactions between the human innate immune system and Candida albicans-understanding and modeling defense and evasion strategies. Frontiers in microbiology. 2015; 6:625. Epub 2015/07/16. https://doi.org/10.3389/fmicb.2015.00625 PMID: 26175718; PubMed Central PMCID: PMC4485224.

17. Sudbery PE. Growth of Candida albicans hyphae. Nature reviews Microbiology. 2011; 9(10):737–48. Epub 2011/08/17. https://doi.org/10.1038/nrmicro2636 PMID: 21844880.

18. Albataineh MT, Kadosh D. Regulatory roles of phosphorylation in model and pathogenic fungi. Medical mycology. 2016; 54(4):333–52. Epub 2015/12/27. https://doi.org/10.1093/mmy/myv098 PMID: 26705834; PubMed Central PMCID: PMC4818690.

19. Day AM, Quinn J. Stress-Activated Protein Kinases in Human Fungal Pathogens. Frontiers in cellular and infection microbiology. 2019; 9:261. Epub 2019/08/06. https://doi.org/10.3389/fcimb.2019.00261 PMID: 31380304; PubMed Central PMCID: PMC6652806.

20. Han T-l, Cannon RD, Villas-Bôas SG. Metabolome analysis during the morphological transition of Candida albicans. Metabolomics: Official journal of the Metabolomic Society. 2012; 8(6):1204–17.

21. Li L, Liao Z, Yang Y, Lv L, Cao Y, Zhu Z. Metabolomic profiling for the identification of potential biomarkers involved in a laboratory azole resistance in Candida albicans. PloS one. 2018; 13(2):e0192328. https://doi.org/10.1371/journal.pone.0192328 PMID: 29394282

22. Noble SM, French S, Kohn LA, Chen V, Johnson AD. Systematic screens of a Candida albicans homozygous deletion library decouple morphogenetic switching and pathogenicity. Nature genetics. 2010; 42(7):590–8. Epub 2010/06/15. https://doi.org/10.1038/ng.605 PMID: 20543849; PubMed Central PMCID: PMC2893244.

23. Evans DR, Stark MJ. Mutations in the Saccharomyces cerevisiae type 2A protein phosphatase catalytic subunit reveal roles in cell wall integrity, actin cytoskeleton organization and mitosis. Genetics. 1997; 145(2):227–41. Epub 1997/02/01. PubMed Central PMCID: PMC1207790. https://doi.org/10.1093/genetics/145.2.227 PMID: 9071579

24. Garbers C, DeLong A, Deruere J, Bernasconi P, Soll D. A mutation in protein phosphatase 2A regulatory subunit A affects auxin transport in Arabidopsis. The EMBO journal. 1996; 15(9):2115–24. Epub 1996/05/01. PubMed Central PMCID: PMC450134. PMID: 8641277

25. Lee CM, Nantel A, Jiang L, Whiteway M, Shen SH. The serine/threonine protein phosphatase SIT4 modulates yeast-to-hypha morphogenesis and virulence in Candida albicans. Molecular microbiology. 2004; 51(3):691–709. Epub 2004/01/21. https://doi.org/10.1111/j.1365-2958.2003.03879.x PMID: 14731272.

26. Furukawa K, Fukuda T, Yamashita SI, Saigusa T, Kurihara Y, Yoshida Y, et al. The PP2A-like Protein Phosphatase Ppg1 and the Far Complex Cooperatively Counteract CK2-Mediated Phosphorylation of Atg32 to Inhibit Mitophagy. Cell reports. 2018; 23(12):3579–90. Epub 2018/06/21. https://doi.org/10.1016/j.celrep.2018.05.064 PMID: 29925000.

27. Banerjee M, Thompson DS, Lazzell A, Carlisle PL, Pierce C, Monteagudo C, et al. UME6, a novel filament-specific regulator of Candida albicans hyphal extension and virulence. Molecular biology of the cell. 2008; 19(4):1354–65. Epub 2008/01/25. https://doi.org/10.1091/mbc.e07-11-1110 PMID: 18216277; PubMed Central PMCID: PMC2291399.

28. Albataineh MT, Lazzell A, Lopez-Ribot JL, Kadosh D. Ppg1, a PP2A-Type protein phosphatase, controls filament extension and virulence in candida albicans. Eukaryotic Cell. 2014; 13(12):1538–47. https://doi.org/10.1128/EC.00199-14 PMID: 25326520

29. Langmead B, Salzberg SL. Fast gapped-read alignment with Bowtie 2. Nature methods. 2012; 9 (4):357–9. Epub 2012/03/06. https://doi.org/10.1038/nmeth.1923 PMID: 22388286; PubMed Central PMCID: PMC3322381.

30. Li B, Dewey CN. RSEM: accurate transcript quantification from RNA-Seq data with or without a reference genome. BMC bioinformatics. 2011; 12:323. Epub 2011/08/06. https://doi.org/10.1186/1471-2105-12-323 PMID: 21816040; PubMed Central PMCID: PMC3163565.

31. Semreen MH, Soliman SSM, Saeed BQ, Alqarihi A, Uppuluri P, Ibrahim AS. Metabolic Profiling of Candida auris, a Newly-Emerging Multi-Drug Resistant Candida Species, by GC-MS. Molecules. 2019; 24 (3). Epub 2019/01/27. https://doi.org/10.3390/molecules24030399 PMID: 30678308; PubMed Central PMCID: PMC6384714.

32. Dieterle F, Ross A, Schlotterbeck G, Senn H. Probabilistic quotient normalization as robust method to account for dilution of complex biological mixtures. Application in 1H NMR metabonomics. Analytical chemistry. 2006; 78(13):4281–90. https://doi.org/10.1021/ac051632c PMID: 16808434

33. Cacciatore S, Tenori L, Luchinat C, Bennett PR, MacIntyre DA. KODAMA: an R package for knowledge discovery and data mining. Bioinformatics. 2017; 33(4):621–3. https://doi.org/10.1093/bioinformatics/btw705 PMID: 27993774

34. Troyanskaya O, Cantor M, Sherlock G, Brown P, Hastie T, Tibshirani R, et al. Missing value estimation methods for DNA microarrays. Bioinformatics. 2001; 17(6):520–5. https://doi.org/10.1093/bioinformatics/17.6.520 PMID: 11395428

35. Wang L, Feng Z, Wang X, Zhang X. DEGseq: an R package for identifying differentially expressed genes from RNA-seq data. Bioinformatics. 2010; 26(1):136–8. Epub 2009/10/27. https://doi.org/10.1093/bioinformatics/btp612 PMID: 19855105.

36. Audic S, Claverie JM. The significance of digital gene expression profiles. Genome research. 1997; 7 (10):986–95. Epub 1997/10/23. https://doi.org/10.1101/gr.7.10.986 PMID: 9331369

37. Kumar L M E.F. Mfuzz: a software package for soft clustering of microarray data. Bioinformation. 2007; 2(1):5–7. Epub 2007/12/18. https://doi.org/10.6026/97320630002005 PMID: 18084642; PubMed Central PMCID: PMC2139991.

38. Subramanian A, Tamayo P, Mootha VK, Mukherjee S, Ebert BL, Gillette MA, et al. Gene set enrichment analysis: a knowledge-based approach for interpreting genome-wide expression profiles. Proceedings of the National Academy of Sciences. 2005; 102(43):15545–50. https://doi.org/10.1073/pnas.0506580102 PMID: 16199517

39. Wishart D, Feunang Y, Marcu A, Guo A, Liang K. vázquez-Fresno R. Sajed T. 2017.

40. Albataineh MT, Kadosh D. Regulatory roles of phosphorylation in model and pathogenic fungi. Sabouraudia. 2015; 54(4):333–52. https://doi.org/10.1093/mmy/myv098 PMID: 26705834

41. Albataineh MT, Kadosh D. Regulatory roles of phosphorylation in model and pathogenic fungi. Med Mycol. 2016; 54(4):333–52. https://doi.org/10.1093/mmy/myv098 PMID: 26705834

42. Offley SR, Schmidt MC. Protein phosphatases of Saccharomyces cerevisiae. Current genetics. 2019; 65(1):41–55. Epub 2018/09/19. https://doi.org/10.1007/s00294-018-0884-y PMID: 30225534; PubMed Central PMCID: PMC6344269.

43. Martin R, Albrecht-Eckardt D, Brunke S, Hube B, Hunniger K, Kurzai O. A core filamentation response network in Candida albicans is restricted to eight genes. PloS one. 2013; 8(3):e58613. Epub 2013/03/22. https://doi.org/10.1371/journal.pone.0058613 PMID: 23516516; PubMed Central PMCID: PMC3597736.

44. Hoyer LL, Payne TL, Hecht JE. Identification of Candida albicans ALS2 and ALS4 and localization of als proteins to the fungal cell surface. Journal of bacteriology. 1998; 180(20):5334–43. Epub 1998/10/10. https://doi.org/10.1128/JB.180.20.5334-5343.1998 PMID: 9765564; PubMed Central PMCID: PMC107581.

45. Almeida RS, Brunke S, Albrecht A, Thewes S, Laue M, Edwards JE, et al. the hyphal-associated adhesin and invasin Als3 of Candida albicans mediates iron acquisition from host ferritin. PLoS pathogens. 2008; 4(11):e1000217. Epub 2008/11/22. https://doi.org/10.1371/journal.ppat.1000217 PMID: 19023418; PubMed Central PMCID: PMC2581891.

46. Eck R, Hundt S, Hartl A, Roemer E, Kunkel W. A multicopper oxidase gene from Candida albicans: cloning, characterization and disruption. Microbiology (Reading). 1999; 145 (Pt 9):2415–22. Epub 1999/10/12. https://doi.org/10.1099/00221287-145-9-2415 PMID: 10517594.

47. Han TL, Cannon RD, Villas-Boas SG. The metabolic basis of Candida albicans morphogenesis and quorum sensing. Fungal genetics and biology: F.G. & B. 2011; 48(8):747–63. Epub 2011/04/26. https://doi.org/10.1016/j.fgb.2011.04.002 PMID: 21513811.

48. Han TL, Cannon RD, Gallo SM, Villas-Boas SG. A metabolomic study of the effect of Candida albicans glutamate dehydrogenase deletion on growth and morphogenesis. NPJ biofilms and microbiomes. 2019; 5(1):13. Epub 2019/04/18. https://doi.org/10.1038/s41522-019-0086-5 PMID: 30992998; PubMed Central PMCID: PMC6453907 non-financial relationships that could be construed as a potential conflict of interest.

49. Fitzmaurice C, Abate D, Abbasi N, Abbastabar H, Abd-Allah F, Abdel-Rahman O, et al. Global, Regional, and National Cancer Incidence, Mortality, Years of Life Lost, Years Lived With Disability, and Disability-Adjusted Life-Years for 29 Cancer Groups, 1990 to 2017: A Systematic Analysis for the Global Burden of Disease Study. JAMA oncology. 2019. Epub 2019/09/29. https://doi.org/10.1001/jamaoncol.2019.2996 PubMed Central PMCID: PMC6777271. PMID: 31560378

50. Hubmann G, Guillouet S, Nevoigt E. Gpd1 and Gpd2 fine-tuning for sustainable reduction of glycerol formation in Saccharomyces cerevisiae. Applied and environmental microbiology. 2011; 77(17):5857–67. Epub 2011/07/05. https://doi.org/10.1128/AEM.05338-11 PMID: 21724879; PubMed Central PMCID: PMC3165387.

51. Lee YJ, Jeschke GR, Roelants FM, Thorner J, Turk BE. Reciprocal phosphorylation of yeast glycerol-3-phosphate dehydrogenases in adaptation to distinct types of stress. Molecular and cellular biology. 2012; 32(22):4705–17. Epub 2012/09/19. https://doi.org/10.1128/MCB.00897-12 PMID: 22988299; PubMed Central PMCID: PMC3486180.

52. Luo S, Hoffmann R, Skerka C, Zipfel PF. Glycerol-3-phosphate dehydrogenase 2 is a novel factor H-, factor H-like protein 1-, and plasminogen-binding surface protein of Candida albicans. The Journal of infectious diseases. 2013; 207(4):594–603. Epub 2012/12/04. https://doi.org/10.1093/infdis/jis718 PMID: 23204165.

53. Desai JV, Bruno VM, Ganguly S, Stamper RJ, Mitchell KF, Solis N, et al. Regulatory role of glycerol in Candida albicans biofilm formation. mBio. 2013; 4(2):e00637–12. Epub 2013/04/11. https://doi.org/10.1128/mBio.00637-12 PMID: 23572557; PubMed Central PMCID: PMC3622937.

54. Desai JV, Cheng S, Ying T, Nguyen MH, Clancy CJ, Lanni F, et al. Coordination of Candida albicans Invasion and Infection Functions by Phosphoglycerol Phosphatase Rhr2. Pathogens. 2015; 4(3):573–89. Epub 2015/07/28. https://doi.org/10.3390/pathogens4030573 PMID: 26213976; PubMed Central PMCID: PMC4584273.

55. Chen YL, Kauffman S, Reynolds TB. Candida albicans uses multiple mechanisms to acquire the essential metabolite inositol during infection. Infection and immunity. 2008; 76(6):2793–801. Epub 2008/02/13. https://doi.org/10.1128/IAI.01514-07 PMID: 18268031; PubMed Central PMCID: PMC2423082.

56. Jin JH, Seyfang A. High-affinity myo-inositol transport in Candida albicans: substrate specificity and pharmacology. Microbiology (Reading). 2003; 149(Pt 12):3371–81. Epub 2003/12/10. https://doi.org/10.1099/mic.0.26644-0 PMID: 14663071.

57. Donalies UE, Stahl U. Increasing sulphite formation in Saccharomyces cerevisiae by overexpression of MET14 and SSU1. Yeast. 2002; 19(6):475–84. Epub 2002/03/29. https://doi.org/10.1002/yea.849 PMID: 11921096.

58. Martin R, Albrecht-Eckardt D, Brunke S, Hube B, Hünniger K, Kurzai O. A core filamentation response network in Candida albicans is restricted to eight genes. PloS one. 2013; 8(3):e58613. https://doi.org/10.1371/journal.pone.0058613 PMID: 23516516

59. Han T-L, Cannon RD, Villas-Bôas SG. The metabolic response of Candida albicans to farnesol under hyphae-inducing conditions. FEMS yeast research. 2012; 12(8):879–89. https://doi.org/10.1111/j.1567-1364.2012.00837.x PMID: 22846172

60. Shareck J, Nantel A, Belhumeur P. Conjugated linoleic acid inhibits hyphal growth in Candida albicans by modulating Ras1p cellular levels and downregulating TEC1 expression. Eukaryotic Cell. 2011; 10(4):565–77. https://doi.org/10.1128/EC.00305-10 PMID: 21357478

61. Sexton JA, Brown V, Johnston M. Regulation of sugar transport and metabolism by the Candida albicans Rgt1 transcriptional repressor. Yeast. 2007; 24(10):847–60. Epub 2007/07/03. https://doi.org/10.1002/yea.1514 PMID: 17605131.

62. Vieira N, Casal M, Johansson B, MacCallum DM, Brown AJ, Paiva S. Functional specialization and differential regulation of short-chain carboxylic acid transporters in the pathogen Candida albicans. Molecular microbiology. 2010; 75(6):1337–54. https://doi.org/10.1111/j.1365-2958.2009.07003.x PMID: 19968788

63. Lorenz MC, Bender JA, Fink GR. Transcriptional response of Candida albicans upon internalization by macrophages. Eukaryotic Cell. 2004; 3(5):1076–87. https://doi.org/10.1128/EC.3.5.1076-1087.2004 PMID: 15470236

64. Buurman ET, Westwater C, Hube B, Brown AJ, Odds FC, Gow NA. Molecular analysis of CaMnt1p, a mannosyl transferase important for adhesion and virulence of Candida albicans. Proceedings of the National Academy of Sciences. 1998; 95(13):7670–5. https://doi.org/10.1073/pnas.95.13.7670 PMID: 9636208

65. García-Carnero LC, Martínez-Álvarez JA, Salazar-García LM, Lozoya-Pérez NE, González-Hernández SE, Tamez-Castrellón AK. Recognition of Fungal Components by the Host Immune System. Current Protein and Peptide Science. 2020; 21(3):245–64. https://doi.org/10.2174/1389203721666191231105546 PMID: 31889486

66. Nelson R, Shibata N, Podzorski R, Herron M. Candida mannan: chemistry, suppression of cell-mediated immunity, and possible mechanisms of action. Clinical microbiology reviews. 1991; 4(1):1–19. https://doi.org/10.1128/CMR.4.1.1 PMID: 2004345

67. West L, Lowman DW, Mora-Montes HM, Grubb S, Murdoch C, Thornhill MH, et al. Differential virulence of Candida glabrata glycosylation mutants. The Journal of biological chemistry. 2013; 288(30):22006–18. Epub 2013/05/31. https://doi.org/10.1074/jbc.M113.478743 PMID: 23720756; PubMed Central PMCID: PMC3724654.